Photosynthetic carbon isotope discrimination and its relationship to the carbon isotope signals of stem, soil and ecosystem respiration

Lisa Wingate[1,2,4], Jérôme Ogée[2], Régis Burlett[2], Alexandre Bosc[2], Marion Devaux[2], John Grace[1], Denis Loustau[2] and Arthur Gessler[3]

[1]School of GeoSciences, University of Edinburgh, Edinburgh EH9 3JN, UK; [2]INRA, UR1263 Ephyse, F–33130 Villenave d'Ornon, France; [3]Institut für Landschaftsstoffdynamik, Leibniz-Centre for Agricultural Landscape Research (ZALF), Eberswalder Straβe 84, D–15374, Müncheberg, Germany; [4]Present address: The Department of Plant Sciences, University of Cambridge, CB2 3EA, Cambridge, UK

Author for correspondence:
Lisa Wingate
Tel: +44 (0)1223 330212
Email: l.wingate@ed.ac.uk

Received: *23 February 2010*
Accepted: *1 June 2010*

New Phytologist
doi: 10.1111/j.1469-8137.2010.03384.x

Key words: $^{13}CO_2$, autotrophic respiration, carbon isotopes, forests, maritime pine, photosynthesis, plant allocation, tuneable diode laser.

Summary

- Photosynthetic carbon (C) isotope discrimination (Δ_A) labels photosynthates (δ_A) and atmospheric CO_2 (δ_a) with variable C isotope compositions during fluctuating environmental conditions. In this context, the C isotope composition of respired CO_2 within ecosystems is often hypothesized to vary temporally with Δ_A.
- We investigated the relationship between Δ_A and the C isotope signals from stem (δ_W), soil (δ_S) and ecosystem (δ_E) respired CO_2 to environmental fluctuations, using novel tuneable diode laser absorption spectrometer instrumentation in a mature maritime pine forest.
- Broad seasonal changes in Δ_A were reflected in δ_W, δ_S and δ_E. However, respired CO_2 signals had smaller short-term variations than Δ_A and were offset and delayed by 2–10 d, indicating fractionation and isotopic mixing in a large C pool. Variations in δ_S did not follow Δ_A at all times, especially during rainy periods and when there is a strong demand for C allocation above ground.
- It is likely that future isotope-enabled vegetation models will need to develop transfer functions that can account for these phenomena in order to interpret and predict the isotopic impact of biosphere gas exchange on the C isotope composition of atmospheric CO_2.

Introduction

Measurements of discrimination against $^{13}CO_2$ during photosynthesis (Δ_A) are useful for assessing the impact of environmental variability on plant metabolism and water relations over daily, seasonal and inter-annual time-frames (Farquhar *et al.*, 1989; Lloyd & Farquhar, 1994). They are also necessary for constraining the influence of terrestrial ecosystems on the atmospheric mass balance of $^{13}CO_2$ (Ciais *et al.*, 1995; Francey *et al.*, 1995; Battle *et al.*, 2000; Randerson *et al.*, 2002). Yet, direct measurements of Δ_A in the field remain sparse (Wingate *et al.*, 2007; Bowling *et al.*, 2008). Instead, a number of different approaches are often employed to estimate plant and ecosystem-scale Δ_A. The most common approach is to either measure or predict the ratio of CO_2 partial pressure in the stomatal cavity relative to that in ambient air (C_i/C_a) and relate this linearly to variations in Δ_A (Farquhar *et al.*, 1982). Alternatively the carbon (C) isotope composition of plant and soil bulk organic matter or CO_2 in air within and above plant canopies are also considered suitable proxies (Keeling, 1961; Kaplan *et al.*, 2002; Baldocchi & Bowling, 2003; Lai *et al.*, 2005; Aranibar *et al.*, 2006). However, these approaches tend to integrate the isotopic signals of post photosynthetic fractionations caused by the construction of biomass or respiratory metabolism and can obscure the relationship between Δ_A and environmental fluctuations (Bowling *et al.*, 2008).

Despite these caveats a number of studies have found correlations between the C isotope composition of

ecosystem-respired CO_2 (δ_E), soil-respired CO_2 (δ_S) and environmental drivers such as relative humidity, temperature, precipitation and soil moisture over daily and monthly time-frames (e.g. (Ekblad & Högberg, 2001; Bowling *et al.*, 2002; Barbour *et al.*, 2005; Ekblad *et al.*, 2005; Knohl *et al.*, 2005; Lai *et al.*, 2005)). These correlations are hypothesized to result from short- to medium-term variations in Δ_A that give rise to detectable variations in the isotopic composition of the metabolic substrates used to fuel respiration (Cernusak *et al.*, 2002; Gessler *et al.*, 2007, 2008). Because it is more practical to measure δ_E than Δ_A for long periods in the field, it would be useful to validate this hypothesized link between Δ_A and δ_E and develop robust ^{13}C transfer functions of ground-based isoflux (defined as the product of a gross CO_2 flux (F_x) and its isotopic composition (δ_x): $I_x = F_x \delta_x$) measurements to the larger-scale measurement and modelling efforts of the atmospheric community.

In addition, it has also been postulated that these temporal correlations between δ_E, δ_S and environmental fluctuations can be used to gauge the 'speed of link' between photosynthetic activity and the transport of C belowground in large trees (Ekblad & Högberg, 2001). Based on monthly measurements over the growing season, Ekblad & Högberg (2001) first demonstrated a 2–4 d lag between atmospheric humidity and the $\delta^{13}C$ of the soil CO_2 flux in chambers for a mature Scots pine forest of 20–25 m height growing in Northern Sweden. Similar results from soil and ecosystem scale measurements using natural abundance concentrations of ^{13}C have since been found for many coniferous and deciduous forests (Bowling *et al.*, 2002; Bhupinderpal-Singh *et al.*, 2003; Steinmann *et al.*, 2004; Barbour *et al.*, 2005; Ekblad *et al.*, 2005; Knohl *et al.*, 2005; Mortazavi *et al.*, 2005; Schaeffer *et al.*, 2008; Marron *et al.*, 2009). More recently, ^{13}C pulse labelling studies have confirmed similar findings (Högberg *et al.*, 2008; Bahn *et al.*, 2009; Plain *et al.*, 2009; Ruehr *et al.*, 2009; Subke *et al.*, 2009). However, there are some field studies that have found no significant correlation between δ_S, δ_E and environmental variables (Bowling *et al.*, 2002; Mortazavi & Chanton, 2002; McDowell *et al.*, 2004; Kodama *et al.*, 2008) indicating an apparent decoupling of the belowground link to recently fixed photosynthates. A clearer explanation of why these biological patterns are occasionally obscured at the soil and ecosystem scale should be sought as they may provide important insights on plant C allocation dynamics below ground in response to environmental stress and phenology.

The purpose of this study was to test directly and for the first time the hypothesis that variations in the C isotope signals of stem, soil and ecosystem respired CO_2 are caused by fluctuations in photosynthetic ^{13}C discrimination observed in the field. This hypothesis was explored by examining the extent of coupling between aboveground and belowground C transfer in tall trees using correlation analysis applied to the natural variations in C isotope signals of CO_2 released by each component of the ecosystem. This was achieved using (1) a novel tuneable diode laser absorption spectrometer (TDLAS), that continuously measured the concentrations of the different CO_2 isotopologues inside branch, stem and soil chambers in addition to the surrounding canopy atmosphere of a maritime pine forest located in France and (2) an isotope-enabled canopy model that allowed us to compare branch chamber measurements with theory and upscale them to the entire canopy. Using this approach we could also explore whether C transfer times between aboveground and belowground organs in tall trees remained static or fluctuated over the growing season in response to environmental conditions or plant allocation patterns, in order to provide an explanation of why some studies observe a strong link between environmental conditions and δ_E, while others do not. Finally this dataset allowed us to test whether isotopic differences between specific component fluxes and corresponding C pools were consistent with post-photosynthetic fractionation theories currently proposed to explain the natural isotopic patterns found in ecosystems, and explore how they affect the C isotope composition of atmospheric CO_2.

Materials and Methods

Site description

The study took place at the Bray experimental site, located at *c.* 20 km from Bordeaux, France (44°42′ N, 0°46′ W, altitude 62 m), in a nearly homogeneous maritime pine stand (*Pinus pinaster* Ait.) planted in 1970. Mean tree height was 20 m and the leaf area index, confined in the top 6 m, was *c.* 3 m^2 m^{-2}. The understorey mainly consists of grass (*Molinia coerulea* L.) whose roots and clumps remain throughout the year but whose leaves are green only from April to late November, with maximum leaf area index and height of 1.4–2.0 m^2 m^{-2} and 0.6–0.8 m, respectively. A 5 cm-thick litter layer composed of compacted grass, dead needles and woody debris remains present all year long. This site has formed part of the CarboEurope and Fluxnet networks since 1996 (Berbigier *et al.*, 2001) and was previously investigated for the C isotope composition of CO_2 during a short study in 1997 (Ogée *et al.*, 2003b, 2004).

Eddy covariance and sapflux measurements

The experimental set-up that provided the meteorological and net ecosystem CO_2 exchange (NEE) measurements used in this study was installed following the requirements of the European project CarboEurope (Berbigier *et al.*, 2001).

A cluster of nine trees were also equipped with sap flow sensors just beneath the live crown, as described in Granier

& Loustau (1994). Raw sap flow data was corrected for stem diameter according to Delzon *et al.* (2004).

TDLAS sampling system

In this study, $^{12}C^{16}O_2$, $^{13}C^{16}O_2$ and $^{12}C^{18}O^{16}O$ concentrations were measured *in situ* using a TDLAS (TGA100A; Campbell Scientific Inc., Logan, UT, USA) housed in an unheated shed at the Bray site. These concentrations were converted to delta notations (and noted $\delta^{13}C$) and are expressed on the VPDB (Vienna Pee Dee Beleminite) scale. The specifications of this analyser for the study of both C and oxygen isotope ratios is described in detail elsewhere (Griffis *et al.*, 2008; Wingate *et al.*, 2010). Further details on the instrument specifications and calibration are provided in the Supporting Information, Methods S1.

A multi-inlet sampling system was designed to automatically select and measure the gas exchange and environmental conditions for one of three different components, including a vertical atmospheric profile below, within and above the canopy (0.1 m, 0.5 m, 1.6 m, 4.8 m, 8 m, 17 m, 19 m, 22.5 m), three open soil chambers or an open stem chamber and a closed branch chamber (Fig. 1). A detailed description of each component is given in Methods S1.

Sampling sequence

Each component as well as calibration tanks were scanned at 1 Hz over a 30-min sampling sequence (Fig. S1). During the experiment this sampling sequence changed slightly depending on how many components were being measured. In brief, at the beginning of every 30-min cycle, each calibration tank was scanned for 60 s (only 30 s at the beginning of the experiment, see Table S1 and Fig S2). The precision of the instrument at reproducing calibration tank values was between 0.3‰ and 0.6‰ for $\delta^{13}C$ and $\delta^{18}O$ (Table S2). The soil chamber manifold was then selected and, over 8 min, the inlet and outlet airstreams of either the stem or of one of the three soil chambers were scanned four times alternatively for a 1-min period. A second scan of the calibration tanks was then repeated as described earlier. The closed dynamic branch chamber was then selected for 5 min. For the initial 150 s the branch chamber was kept open and ventilated to establish the initial concentration. This was followed by a final scan of the calibration tanks, before scanning each inlet of the ecosystem profile for 60 s each. Each soil chamber was revisited and scanned every 2.5 h. An example of our sampling sequence can be seen in Methods S1, Fig. S1 alongside details of our calibration, data averaging and filtering procedure (see Figs S2–S4).

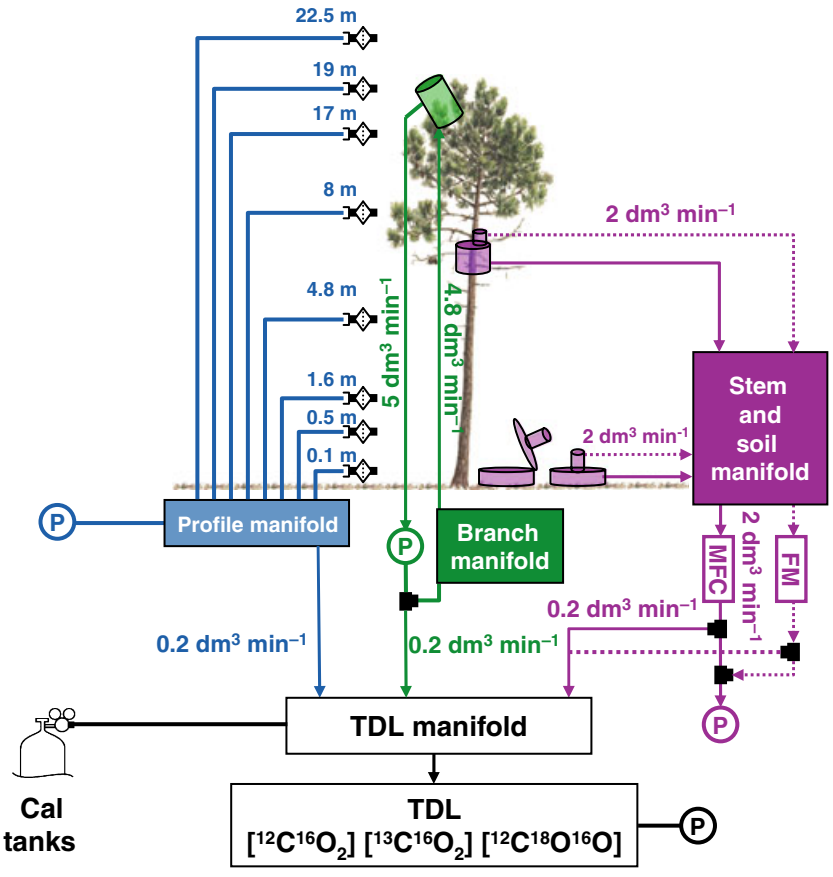

Fig. 1 Experimental set-up used to measure the isotope signals of CO_2 exchanged between forest ecosystem components and the atmosphere that included the routine measurement of one branch, one stem and three soil chambers. MFC, mass flow controller; FM, flow meter; P, pump.

Carbon isotope composition of the net CO_2 flux from branch, soil and stem chambers

Branch CO_2 flux (F_A) was calculated from the rate of change in total CO_2 mixing ratio observed in a branch chamber between 0 and 60 s after closure (Wingate *et al.*, 2010). Net branch isotope discrimination Δ_A was calculated over the same 60-s period according to (McNevin *et al.*, 2006):

$$\Delta_A = \frac{d\,(\log_e[^{12}CO_2])}{d\,(\log_e[^{13}CO_2])} - 1 \qquad \text{Eqn 1}$$

A linear regression between $\log_e[^{12}CO_2]$ and $\log_e[^{13}CO_2]$ was performed and when the correlation coefficient was < 0.98 the data were discarded from further analysis. The C isotope signal of the net branch CO_2 flux was then calculated from the data as $\delta_A = (\delta_a - \Delta_A)/(1 + \Delta_A)$, where δ_a is the C isotope composition of atmospheric CO_2 surrounding the foliage inside the chamber while ventilated.

For each stem or soil chamber, the steady-state net CO_2 flux F_W and F_S, respectively, and its C isotope signal (δ_w and δ_S, respectively) was calculated using a simple isotopic mass balance (Wingate *et al.*, 2008; Maseyk *et al.*, 2009). For example, for soil chambers, $F_S = u(C_o - C_e)/S$ and:

$$\delta_S = \frac{\delta_o C_o - \delta_e C_e}{C_o - C_e} \qquad \text{Eqn 2}$$

(u is the flow rate of air through the chamber (2 dm^{-3} min^{-1} for the soil and 2 dm^{-3} min^{-1} until day 268 and 1 dm^{-3} min^{-1} thereafter for the stem); S is the surface area of the chamber (0.07 m^2 for the soil and 0.09 m^2 for the stem); C_o, C_e and δ_o, δ_e are the mole fractions and C isotopic compositions of CO_2 in the air leaving and entering the chamber, respectively). For each measurement, four replicates were performed (see Fig. S1) and used to calculate a standard deviation for F_S and δ_S.

Carbon isotope composition of ecosystem respiration from canopy profiles

For each night, the C isotope composition of ecosystem respired CO_2 (δ_E) was determined from the 'instant' slope of the regression between the product $C_a\delta_a$ and C_a (Bakwin *et al.*, 1998; Miller & Tans, 2003; Ogée *et al.*, 2003b) using measurements from 01:00 h until dawn. All air profile levels were included as well as soil chamber inlets in order to increase the number of measurements close to the ground, and an orthogonal distance regression was used to account for errors both on δ_a and C_a (taken as the standard deviation of the mean for each measurement). Regression analysis was restricted to those nights where the CO_2 concentration range exceeded 60 μmol mol^{-1} (Zobitz *et al.*, 2006).

Carbon isotope composition of ecosystem C pools

Needle samples were collected monthly from three locations in the upper canopy, pooled in glass containers and frozen in the field. In the laboratory, samples were then freeze-dried, ground and weighed into tin cups for $\delta^{13}C$ analysis of bulk organic matter (BOM). Isotope ratio mass spectrometer (IRMS) analysis was completed on a Delta V mass spectrometer coupled online to a FlashEA elemental analyser (both Thermo Scientific, Bremen, Germany) at the Leibniz-Centre for Agricultural Landscape Research (ZALF). Precision was 0.1‰. This ground material was also used to obtain the $\delta^{13}C$ composition of the water-soluble organic matter (WSOM) fraction of needles following the method described by Brandes *et al.* (2006).

The $\delta^{13}C$ composition of phloem WSOM was also analysed on phloem discs sampled monthly at breast height. From this analysis we obtained information on the $\delta^{13}C$ composition of total extracts as well as those of glucose and sucrose. Full details of these analyses are provided in Devaux *et al.* (2009).

In addition, two tree cores were taken at breast height at the end of the experiment to obtain the cellulose deposited in the 2007 tree ring. This core was sliced using a microtome, lignin was extracted from the whole wood and the cellulose was purified and analysed for its $\delta^{13}C$ composition following the procedure described in Ogée *et al.* (2009).

Finally, litter and soil samples were collected on two occasions during April and August 2007 at six different locations nearby the soil chambers for each date. The soil samples were collected at six depths for each location (0–5, 5–10, 10–15, 15–20, 20–25 and 25–30 cm depth). The samples were dried, ground and weighed into tin cups for $\delta^{13}C$ analysis using an elemental analyser (CE Instruments NA2500 Elemental Analyser, CE Instruments, Wigan, UK) connected to a dual inlet IRMS (VG Prism, Micromass, Manchester, UK) at the School of GeoSciences in The University of Edinburgh, UK. Precision was 0.1‰.

Representativeness of chamber-based estimates

Because of restricted canopy access, we were unable to install more than one branch chamber in the canopy. For a number of reasons we decided to place this branch chamber on an entire 1-yr-old shoot near the top of the canopy. For this forest, 1-yr-old shoots have been found to contribute the largest photosynthetic surface area to the total foliage surface area (*c.* 48%, see Porté *et al.* (2000)) and exhibit the largest CO_2 assimilation rates (Porté & Loustau, 1998). Furthermore, because these shoots are also located on the outer edges of the crown they are relatively unshaded compared with the older shoots.

Because of these sampling limitations we calculated Δ_A (see Methods S1 for further details) using the isotope-

enabled multilayer canopy model MuSICA (Ogée *et al.*, 2003a,b, 2004) to verify whether the temporal patterns and absolute values of observed Δ_A were similar to those predicted by theory. This was completed for both 1-yr-old sun shoots and the whole canopy in order to compare with branch chamber observations and verify the representativeness of 1-yr-old shoot measurements. This model has been validated against several gas-exchange and isotope datasets in this forest (Ogée *et al.*, 2003a,b, 2004) and is therefore a highly suitable tool for this analysis.

Stem chamber measurements during 2007 were also limited to one tree and height beneath the canopy. However, in 2008 we also performed similar stem chamber measurements at two heights and on three different trees and found very consistent isotopic signals and flux rates between all the chambers (M. Devaux *et al.*, unpublished data).

Lastly, three soil chambers were used throughout the entire study period to estimate the average soil CO_2 efflux rate and corresponding C isotope composition. In the following, standard deviations on soil chamber data represent the spatial variability between these three soil chambers.

Results

Seasonal patterns in component CO_2 fluxes

The meteorological conditions experienced by our maritime pine forest during the 2007 growing season are shown in Fig. 2. This growing season was characterized by mild temperatures that rarely fell below 0°C and relatively humid conditions, with moderately high vapour pressure deficits (VPD) occurring in April and occasionally during July to September. Rainfall was almost evenly distributed throughout the year, although the end of the growing season (September–November) received comparatively less rain, leading to a moderate soil water deficit. These weather conditions could have been ideal for C uptake by the vegetation, had incoming radiation not been limiting, especially in May and August. Indeed the forest was a net sink for C between the months of March and October (Fig. 3), but a couple of synoptic events did cause the ecosystem to lose C to the atmosphere. The most striking period occurred at the end of August when a weather system releasing a substantial amount of rain passed through, reduced incoming radiation and recharged soil water slightly (shaded panel in Fig. 3). Inspection of the chamber flux data indicates that an increase in soil respiratory losses primarily led to this ecosystem becoming a source of CO_2 to the atmosphere (Fig. 3). The observed net ecosystem exchange (NEE) of CO_2 did not, however, display exactly the same shape as the soil flux data but rather consisted of a 'double hump'. This particular pattern seems to have resulted from dynamic variations in the day-to-day rates of photosynthesis by the canopy. This is

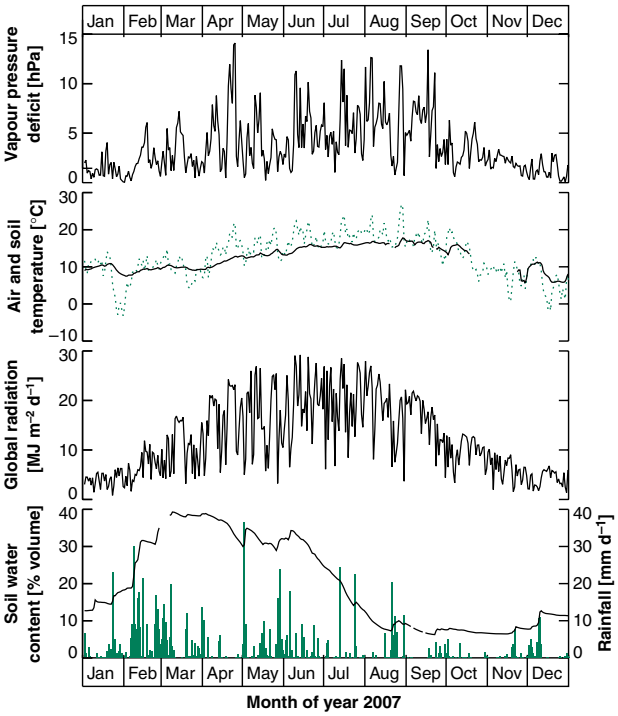

Fig. 2 Seasonal variations in mean daily vapour pressure deficit, air temperature (dotted line), soil temperature (solid line), global radiation, soil water content and rainfall (solid bars) during the 2007 growing season.

most clearly illustrated by the modelled photosynthetic rate that shows a strong reduction before the increase in the soil CO_2 efflux. However, this temporary reduction in F_A is not apparent in the observed 5-d running mean shown in Fig. 3 because low rates of photosynthesis, not predicted by our model, were already observed before the rainy period. This unsettled weather was sharply replaced by more persistent warm, clear and dry conditions that led to a recovery of the C sink status with increased levels of photosynthetic activity displayed by the data and the model. Immediately after the rainy period (end of the shaded area in Fig. 3) both CO_2 assimilation and transpiration rapidly dropped to rates lower than those observed before the rainy period, indicating that our branch and forest may have been experiencing a certain degree of water stress. A similar situation seems likely to have occurred again at the beginning of October although system failures restrict any detailed analysis of the interactions between photosynthesis and respiration during this other period.

Diurnal and seasonal patterns in branch photosynthetic discrimination

Diurnal and seasonal patterns of branch ^{13}C discrimination (Δ_A) measured over the 2007 growing season are presented in Fig. 4. Over this period the majority of daytime Δ_A values ranged between 10‰ and 35‰. The highest values

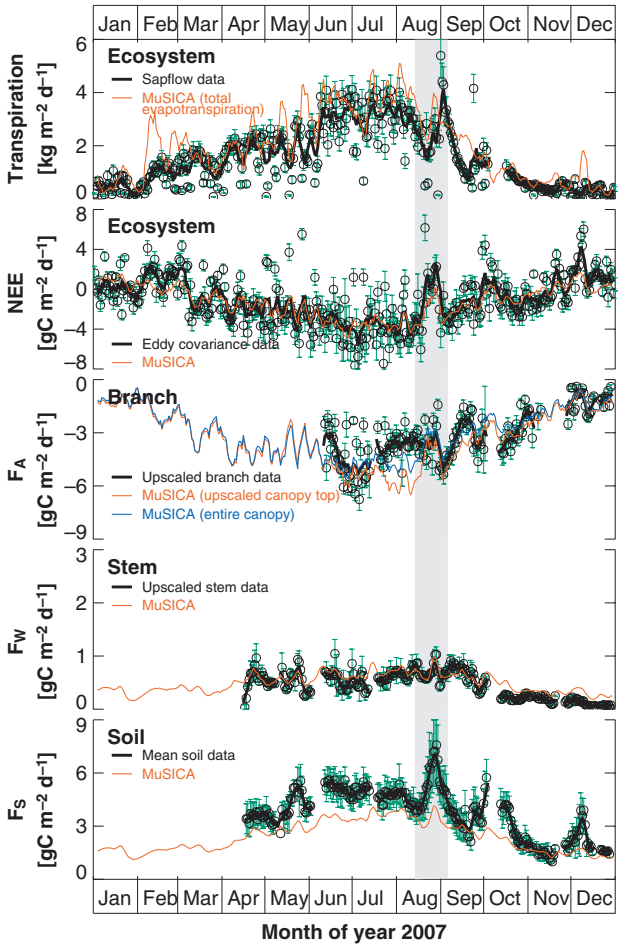

Fig. 3 Seasonal variations in the observed mean daily (circles) or 5-d running mean (thick solid black lines) of sap flux-derived transpiration rates, modelled ecosystem evapotranspiration rates (thin red line) (includes canopy, soil and understorey contributions) and net CO_2 exchange measured and modelled (thin red line) at the ecosystem (NEE), branch (F_A), stem (F_W) and soil (F_S) scale during 2007. Branch fluxes are shown for daytime conditions only and are expressed on a ground area basis using the total canopy leaf area predicted by the model. Modelled branch fluxes are for either the entire canopy (thin blue line) or a canopy of 1-yr-old shoots only (thin red line).

of Δ_A typically occurred at dusk throughout the growing season, but also in the early mornings of June and July and throughout the day during the winter months. This generally led to an asymmetric daily pattern in Δ_A with highest values occurring when CO_2 uptake was low, indicating a relatively high proportion of CO_2 molecules being respired that could contain a slightly different isotopic composition to that of current assimilates (Wingate *et al.*, 2007).

During June and the start of July when weather conditions were still relatively wet and cloudy, midday Δ_A values tended to be high (> 15‰) with lower values observed only occasionally. By contrast, the end of July and the months of August and September gave rise to much lower midday Δ_A values (often < 15‰), when soil moisture contents were relatively lower than those observed earlier in the season. (Figs 2 and 4). Rain events during this study often caused values of Δ_A to increase above 20‰ and are often identified as conspicuous orange and red regions, for example, during the rainy periods of August and December.

Seasonal patterns in the $\delta^{13}C$ of component CO_2 fluxes

During the summer months (July–September), the $\delta^{13}C$ signal of both stem and soil respired CO_2 were generally more depleted than the observed flux-weighted daytime photosynthetic signal $\delta_A = (\delta_a - \Delta_A)/(1 + \Delta_A)$ (Figs 5 and 6). Outside this period, they both remained in the same range of values as observed δ_A. However, model simulations

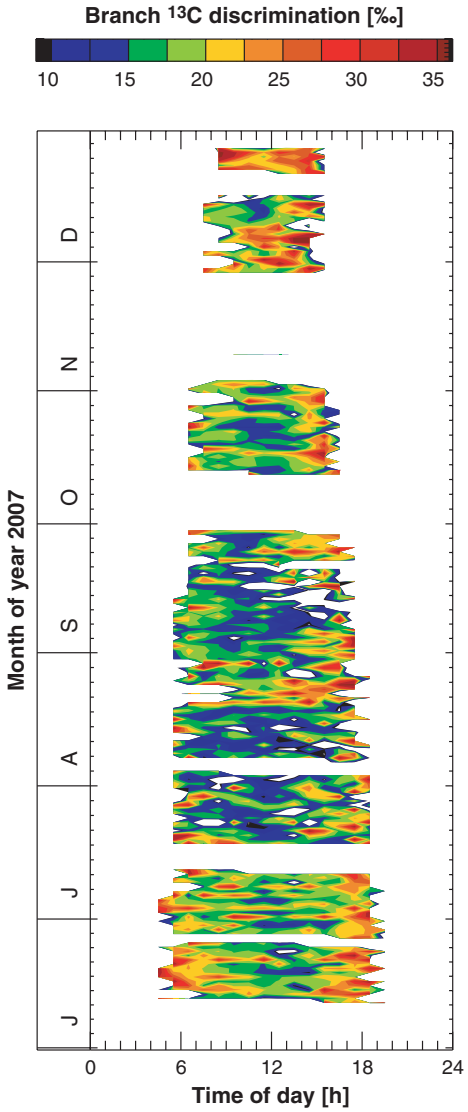

Fig. 4 Diurnal and seasonal variations in branch ^{13}C discrimination (Δ_A) measured during 2007 in the maritime pine forest studied.

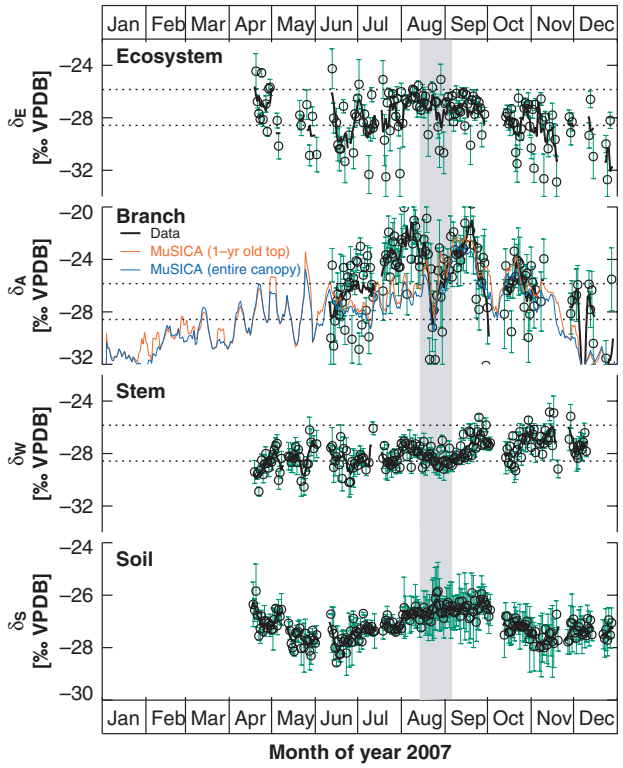

Fig. 5 Seasonal variations in the flux-weighted daily carbon isotope signals (circles) of ecosystem respiration, branch photosynthesis, stem respiration and soil respiration alongside their 5-d running mean value (thick solid black line) during 2007 in a maritime pine forest. Branch observations are plotted alongside model predictions for 1-yr-old shoots at the top of the canopy (thin red line) and for the entire canopy (thin blue line). Note that branch data are for daytime conditions only, ecosystem signals were determined from night-time profiles between 01:00 h and dawn and soil and stem signals represent daily signals. Dotted lines in the top three panels indicate the range of δ_S values observed over the measurement period.

for both 1-yr-old shoots and the entire canopy predicted that δ_A during June and July could have been somewhat more depleted than the observed values and somewhat closer to those signals observed by the stem and soil chambers. It remains unclear why the branch chamber results are different from those modelled during June and July while both give similar results outside this period. The tree installed with both the branch and stem chamber exhibited similar sap flow rates and responses to environmental fluctuations to those observed for other trees in the same stand, indicating that at least the tree containing the chambers was not particularly unusual from any other nearby. In the following text, we therefore use the modelled and observed photosynthetic signals as potential upper and lower estimates of δ_A during this particular period.

Over the entire measurement period, we found that δ_W and δ_S varied by *c.* 4‰ and 3‰, respectively, and that the soil signal tended to be slightly more enriched than the stem, especially in April and August (Fig. 5). Over the season, δ_S exhibited a progressive enrichment between June and September of *c.* 3‰, and then became rapidly depleted, reaching a minimum in November. This is generally consistent with the low-frequency Δ_A and δ_A variations measured and predicted for the branch over the same timeframe (Figs 4 and 5). However, the enriched values in δ_S before branch chamber observations during April and May do not seem to be linked to the low-frequency variations in δ_A predicted by MuSICA (Fig. 5).

We also found that δ_W, more than δ_S, often displayed shorter-term (synoptic) variations that appeared attenuated but coupled to the variations in δ_A. This is most obvious over the period before, during and after the rains in August. Before the rain events, relatively high VPDs coincided with enriched estimates of δ_A at *c.* −22‰ VPDB. Thereafter, a gradual decrease in VPD, followed by a period of wet and overcast conditions caused observed and modelled δ_A signals to drop dramatically by *c.* 7‰ and 4–5‰, respectively. When warmer and drier conditions returned after the rain events, observed and modelled δ_A signals returned to values of *c.* −21‰ VPDB. During these variations of VPD the stem isotopic signal also followed a similar pattern to δ_A but with a much smaller amplitude of only 2‰, and a minimum value of *c.* −29‰ VPDB. By contrast, δ_S appeared to be decoupled from the short-term canopy dynamics of this synoptic event (Fig. 5). Indeed, during the first days of the rainy period, while all other components of the ecosystem were becoming depleted, the soil flux signal became relatively more enriched, coinciding with the maximum soil CO_2 efflux rates (Fig. 3). At other times, however, both δ_W and δ_S seemed to follow synoptic variations in δ_A. For example, during the rainy period at the end of September, δ_A, δ_W and δ_S systematically shifted in the same direction to more depleted values (Fig. 5).

At the ecosystem scale, the $\delta^{13}C$ of respired CO_2 (δ_E) measured during the night was similar in absolute value and range to the soil and stem signals measured between the months of July to October (Fig. 5). The overall seasonal pattern of the ecosystem signal was generally similar to that of the soil, displaying a gradual enrichment over the summer months and becoming more depleted from October onwards. However, the frequency of δ_E isotopic shifts was relatively higher than those observed for δ_W and δ_S and tended to be greater, between 3‰ and 4‰.

Comparison of $\delta^{13}C$ component CO_2 fluxes with plant and ecosystem C pools

The range of $\delta^{13}C$ variations for these different CO_2 flux signals over the 'summer' months (from 21 June to 21 October) were also compared with the C isotope composition of a variety of plant and ecosystem C pools measured for the same period (Fig. 6). The observed summer $\delta^{13}C$ signal of branch photosynthesis was, on average, −24.7‰

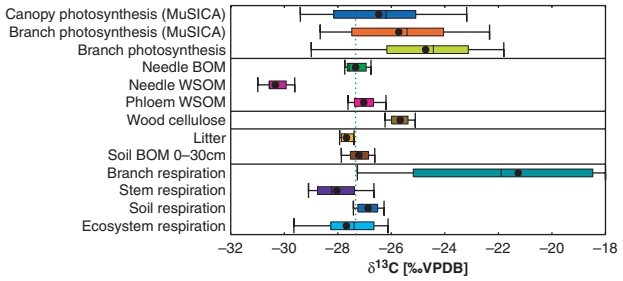

Fig. 6 Synthesis showing the $\delta^{13}C$ composition of the various pools and CO_2 fluxes measured and modelled in the maritime pine site during the 2007 measurement period (from 21 June to 21 October). Circle represents the mean, the box represents the median and 25% upper/lower quartiles and the tails represent the 10% and 90% limits of the data.

VPDB, while model estimates for this signal were somewhat more depleted (at −25.7‰ and −26.5‰ VPDB for 1-yr-old shoots at the top of the canopy and the entire canopy, respectively), because of the model-data disagreement in July and early August already noted in Fig. 4. This mean observed branch value was more enriched than any other flux or C pool in the ecosystem with the exception of the nocturnal branch respiration flux that was, on average, at −21.3‰ VPDB. This was not the case for the modelled canopy-integrated photosynthetic signal that was, on average, slightly more depleted than wood cellulose (at −25.7‰ VPDB) and very close to the soil flux signal (−26.9‰ VPDB). Although the observed $\delta^{13}C$ of branch photosynthesis was, on average, more enriched than the other components measured during the same period, its variability over the season was large and encompassed the range of $\delta^{13}C$ values for all metabolites and C pools, with the exception of the WSOM fraction extracted from needles that was very depleted at −30.3‰ VPDB. The $\delta^{13}C$ of the stem phloem WSOM fraction was, on average, −27.0‰ VPDB and fell between the values for the $\delta^{13}C$ of stem CO_2 flux (−28.0‰ VPDB) and stem cellulose (−25.7‰ VPDB). Also, soil organic matter (SOM) and soil litter $\delta^{13}C$ signals were, on average, −27.2‰ VPDB and −27.7‰ VPDB, respectively – both very similar to the $\delta^{13}C$ signals of the soil CO_2 flux and the stem phloem WSOM fraction. On average, and over the same period, the ecosystem respiration signal δ_E was also depleted compared with the photosynthetic signal, at −27.7‰ VPDB, and lay between the soil and stem respiratory signals.

Time lag analysis

To further explore the fate of newly assimilated C transfer within the tree and its eventual return to the atmosphere we calculated the Spearman's correlation coefficients between time-series of VPD, observed δ_A or modelled δ_A and those from the respired $\delta^{13}C$ signals. For that, we used the 5-d running mean time-series shown in Fig. 5 and computed correlation coefficients between VPD, observed δ_A or modelled δ_A and the other time-series using a 45-d moving window for different time lags (1–14 d). Over this 45-d window at least 50% of the data were required to calculate a correlation coefficient. Results from this analysis are shown in Fig. 7, where red areas indicate a high degree of positive correlation with observed δ_A, modelled δ_A or VPD.

This correlation analysis indicated that the stem respiration signal δ_W was tightly coupled with VPD and δ_A over most of the study period. However the number of days that δ_W lagged behind the photo-assimilate or VPD signal varied from *c.* 2–3 d in August to 8–12 d in September, with somewhat different seasonal patterns in lag times depending on the time series used as a reference. Correlation analysis using the observed δ_A signal also indicates a 12-d lag in δ_W in June and a relatively persistent lag of *c.* 6 d at the end of the observation period, while correlation analysis using the modelled δ_A and VPD signals both indicate longer time lags during the budburst period in April followed by much shorter time lags during the growing season from May to July, that increase again at the end of the summer months.

Correlation analysis between δ_A (or VPD) and δ_S also displayed variable time lags over the observation period, but also indicated periods, associated with cloudy and rainy conditions (e.g. June and August), when the two signals were either weakly or anticorrelated (in June this is not true for the observed δ_A signal but this may be result from the lack of data earlier in May required to perform the correlation analysis over the entire 45-d window). During other periods, a lag between observed δ_A and δ_S of between 6 and 10 d in July and September and down to 3–5 d in October was observed.

At the ecosystem scale the degree of coupling between δ_A (or VPD) and δ_E exhibited time lags similar to those observed for δ_S, except in August when δ_S became decoupled to δ_A and time lags for δ_E became similar to those observed for δ_W.

Discussion

Fractionation during autotrophic and heterotrophic respiration

Our study showed a strong enrichment (3–4‰ on average) in branch-respired CO_2 compared with the photosynthetic signals and even stronger when compared with the needle WSOM fraction (Fig. 6). This pattern is consistent with previous observations for autotrophic organs (Tcherkez *et al.*, 2003; Badeck *et al.*, 2005; Bathellier *et al.*, 2007; Bowling *et al.*, 2008) and the theory that ^{13}C-enriched CO_2 is preferentially released from the C-4 position of glucose by the pyruvate dehydrogenase (PDH) complex and contributes strongly to the total respiratory flux from leaves

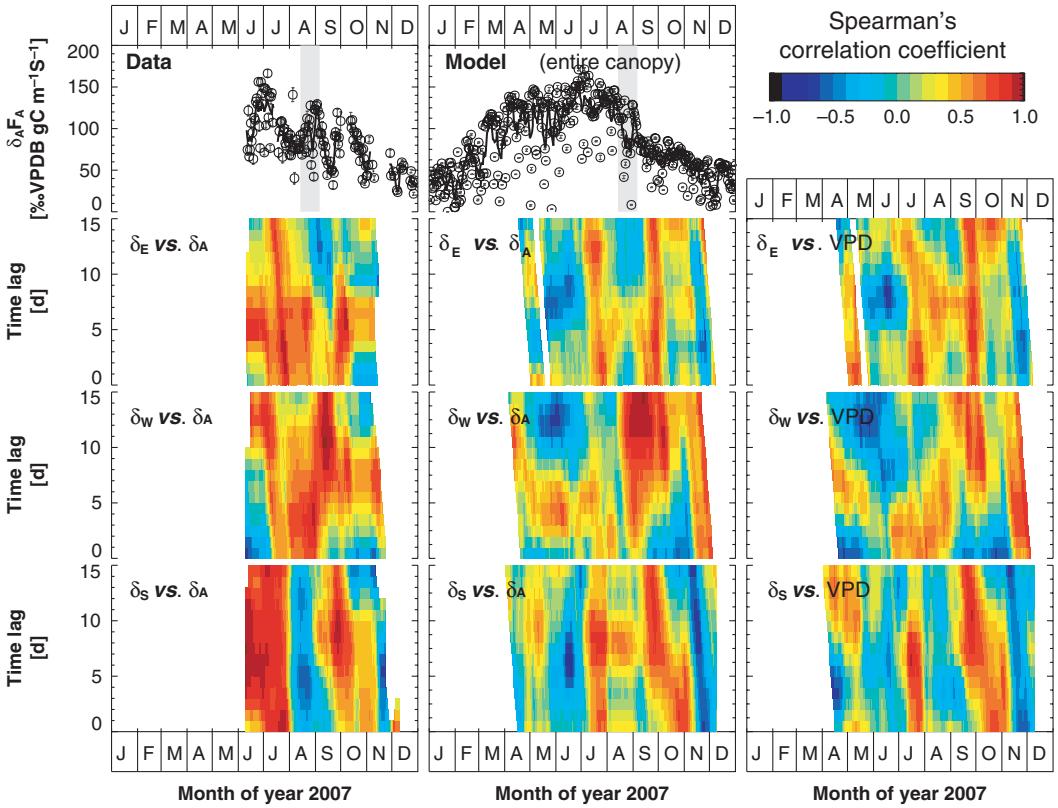

Fig. 7 Seasonal variations in the measured daytime branch isoflux scaled to the canopy and modelled daytime whole-canopy isoflux alongside the correlation strength between the daily carbon isotope signal from observed branch photosynthesis, modelled canopy photosynthesis or daily vapour pressure deficit against that of ecosystem, stem and soil respired CO_2 with varying lag times. N.B. the isoflux is defined as the product of a gross CO_2 flux (F_x) and its isotopic composition (δ_x): $I_x = F_x\ \delta_x$, and branch data are for daytime conditions only.

in the dark (Rossman *et al.*, 1991; Tcherkez *et al.*, 2004; Bathellier *et al.*, 2007; Wingate, 2008). In addition, $\delta^{13}C$ of triose phosphates diverted into starch storage during the day are relatively ^{13}C-enriched causing a diel variation in $\delta^{13}C$ of glucose that contributes to the ^{13}C-enriched flux signal of CO_2 respired at night (Gleixner *et al.*, 1993; Gleixner & Schmidt, 1997; Tcherkez *et al.*, 2004; Gessler *et al.*, 2008).

Our results also showed that $\delta^{13}C$ of stem-respired CO_2 was depleted (by 2–4‰ on average) compared with that of δ_A, the phloem WSOM fraction and wood cellulose (Figs 5 and 6). This finding is in contrast with most observations of respired CO_2 from woody stems, where the CO_2 released by stems in the dark is generally ^{13}C-enriched relative to the whole tissues and/or putative substrates (Cernusak *et al.*, 2001; Damesin & Lelarge, 2003; Gessler *et al.*, 2007; Kodama *et al.*, 2008). Our observations are, however, consistent with investigations made on other heterotrophic organs such as roots (Badeck *et al.*, 2005; Klumpp *et al.*, 2005; Bathellier *et al.*, 2007) and stems (Gessler *et al.*, 2009). Our results could indicate that the refixation of CO_2 by phosphoenol pyruvate corboxylase (PEPC) (anaplerotic uptake) that fractionates by 5.7‰ in favour of ^{13}C and leads to an overall depletion of CO_2 remaining in the stem (Melzer & O'Leary, 1987), is important in maritime pine.

Lignin synthesis could also result in the release of ^{13}C-depleted CO_2 from woody stems. The building blocks of lignin are synthesised in plastids by the pentose phosphate pathway (PPP) and can constitute up to 30% of maritime pine wood (Bert & Danjon, 2006). The CO_2 released during the oxidative stage of this pathway is known to originate from the C-1 position of glucose which is relatively ^{13}C-depleted. In roots the contribution of the PPP to the total CO_2 efflux can be substantial (*c.* 25%) (Dieuaide-Noubhani *et al.*, 1995; Bathellier *et al.*, 2008). However, it remains unclear how important the contribution of this pathway is to the total CO_2 efflux in woody stems and how the contribution varies over the growing season.

Unlike δ_W, the average $\delta^{13}C$ of soil-respired CO_2 was comparable to that of total phloem WSOM extracts (Fig. 6). From previous observations on trenched and untrenched plots in mature maritime pine stands near our site, root respiration represents *c.* 40% of the total soil CO_2 efflux (R Burlett, *et al.*, unpublished). If we assume that the $\delta^{13}C$ of root-respired CO_2 has the same composition as

stem respiration (−28.5‰), to obtain a total soil CO_2 efflux signal of *c.* −26.5‰ would require a ^{13}C-enriched contribution of −25.2‰ via heterotrophic respiration. This enriched signal is consistent with the observation during the rainy period of a small enrichment in δ_S while the autotrophic components were becoming depleted, perhaps indicating an enhanced heterotrophic contribution. If the substrate for heterotrophic respiration is soil BOM, our results indicate a modest fractionation of *c.* +2‰ during heterotrophic respiration, consistent with results for microbial studies (Andrews *et al.*, 2000).

Our study also found a strong depleted signal in the needle WSOM fraction compared with all other ecosystem C pools or CO_2 fluxes (Fig. 6). This result followed the pattern whereby $\delta^{13}C$ of the WSOM fractions in leaf < twig phloem < stem phloem at 1.3 m (Damesin & Lelarge, 2003; Brandes *et al.*, 2006; Gessler *et al.*, 2007; Kodama *et al.*, 2008; Hu *et al.*, 2010). The mechanism for this consistent pattern of ^{13}C enrichment in sugars downstream of the leaf remains unclear, although a number of interesting hypotheses have been postulated (for a review see Cernusak *et al.*, 2009).

The pattern between $\delta^{13}C$ of observed and modelled photosynthetic fluxes, needle BOM and the needle WSOM fraction is, however, unusual. Many studies have found more depleted $\delta^{13}C$ in foliage BOM than in the foliage WSOM fraction, and individual sugars (Bowling *et al.*, 2008; Cernusak *et al.*, 2009), but a few studies (including ours) also indicate that this pattern is not always found (Badeck *et al.*, 2009; Sun *et al.*, 2009). It could be that the WSOM fraction we extracted contains a large concentration of ^{13}C-depleted compounds such as amino and organic acids. Previous studies indicate that such acids in foliage WSOM extracts are often negligible (Brandes *et al.*, 2006; Gessler *et al.*, 2009). A large contribution of polyols such as pinitol and myo-inositol might also be at the origin of this pattern. These compounds are known to accumulate in maritime pine needles during drought stress (Nguyen & Lamant, 1988) and are typically 2–3‰ more depleted than glucose and sucrose (Devaux *et al.*, 2009). These polyols tend not to be used in the construction of biomass or dark respiration (Smith & Phillips, 2010), explaining a weaker ^{13}C depletion in needle BOM and branch respiration (Fig. 6).

Fate of newly assimilated C within the ecosystem

Using natural abundance gas-exchange techniques in the field, it can be challenging to detect the turnover time of C at the plant and ecosystem scale. Unlike pulse labelling experiments where only a few hours of labelling are required to imprint the C pool of large trees (Högberg *et al.*, 2008; Bahn *et al.*, 2009; Plain *et al.*, 2009; Ruehr *et al.*, 2009; Subke *et al.*, 2009), natural abundance experiments require both large C fluxes associated with strong shifts in the isotopic inputs (i.e. large isofluxes) and for those shifts to persist over a number of days. For example, during the rainy period of August there was a very strong depletion in the isotopic signal of the photosynthetic flux accompanied by low rates of CO_2 assimilation that led to a reduction in the isofluxes (Fig. 7, top panels). Thus, this strong isotopic signal carried by a relatively small amount of C is likely to have been diluted in the larger existing C pool of the plant and furthermore by the heterotrophic contributions of the total soil CO_2 flux, compromising the detection of this isotopic shift at the soil scale.

Performing correlation analysis between multiple components in an ecosystem and obtaining a strong degree of coupling also requires that the $\delta^{13}C$ produced by respiring organs or organisms is primarily regulated by the isotopic variations of δ_A. However, if substrates with a $\delta^{13}C$ different from δ_A are used for metabolism, the coupling would be reduced (Bhupinderpal-Singh *et al.*, 2003). Similarly, if the metabolic pathways involved in producing CO_2 during respiration fractionate differently in response to changes in environmental conditions then this could also confound the correlation. Our results indicate that post-photosynthetic fractionations may occur and that the signals of respiration may differ from δ_A. Such caveats have been highlighted by other studies (Kodama *et al.*, 2008; Gessler *et al.*, 2009).

Nonetheless, our correlation analysis (Fig. 7) still revealed strong responses of stem-, soil- and ecosystem-respired $\delta^{13}C$ signals to changes in observed and modelled photosynthetic discrimination over the season. We also found strong correlations with VPD alone indicating that VPD may be a reasonable proxy to gauge the 'speed of link' between aboveground and belowground C transport in the absence of Δ_A measurements, especially for stem measurements. During the rainy period (highlighted in Figs 5 and 7), the depleted isotopic signal of δ_A was transferred to the CO_2 respired by the stem, but no similar depletion was observed from the soil (Fig. 5), resulting in a weak correlation between δ_S and observed δ_A (or VPD) (Fig. 7). We hypothesize that this reduction in correlation was caused by an increase in the contribution of heterotrophic respiration to the total soil CO_2 flux with a ^{13}C-enriched signal and a small flux of C (relative to the total soluble C pool) into the tree carrying the depleted signal. In addition, when we extended the time-series available for correlation analysis using modelled δ_A and VPD we found another period during June when the coupling with δ_S was anti-correlated with these two signals (Fig 7). We speculate that active shoot and wood growth curtailed the supply of freshly assimilated C below ground, forcing roots to sustain their metabolic requirements with reserve carbohydrates. These explanations could help explain why some previous isotopic studies at lower temporal resolution or for shorter periods have not found evidence of strong coupling between

canopy photosynthesis and ecosystem respiration (Bowling *et al.*, 2002; Mortazavi & Chanton, 2002; McDowell *et al.*, 2004; Kodama *et al.*, 2008).

Given the distance between our branch, stem and soil chambers (*c.* 4 and 20 m, respectively) our lag time analysis indicates transport velocities of between 0.03 m h^{-1} in spring and autumn and 0.14 m h^{-1} in summer. Further experiments performed in 2008 using multiple stem chambers at different heights in the canopy further confirm this range of transport velocities (M Devaux *et al.*, unpublished). These transport velocity values are at the lower range of transport velocities calculated for a range of plant functional types and sizes (Mencuccini & Höltta, 2009). A possible explanation could be that the sieve pores of gymnosperms are generally much smaller than those of angiosperms (< 0.8 μm) (Schulz, 1992; Schulz & Thompson, 2001) and are covered on either side by extensive lengths of endoplasmic reticulum (ER) membrane (Neuberger & Evert, 1974; Schulz, 1992). These ER complexes appear to be important obstacles to mass flow and seem to exclude a strictly passive translocation down a concentration gradient in gymnosperms, as often described by the Münch hypothesis (Münch, 1930). Interestingly, using a numerical model of the Münch theory, Mencuccini & Höltta (2009) found it necessary to increase the specific conductivity and turgor pressure differences in tall trees to match the observed velocities derived from their literature review, indicating that slower transfer rates are theoretically anticipated.

We also found that the transport velocities between Δ_A (or VPD) and the respired CO_2 signals appeared to vary over the season. Again we speculate that the allocation of C within the plant may alter in response to the C sink strength of growing organs over the season. Changes in source-to-sink relations that occur over the year (Kozlowski, 1992) are known to strongly influence mass flow of sugars in the phloem (Peuke *et al.*, 2006). An alternative explanation could be that drought stress can reduce the downstream transport of sugars in trees. Ruehr *et al.* (2009) recently demonstrated that drought stress reduced transport rates from 0.5–1.0 m h^{-1} (Keitel *et al.*, 2003) to 0.1 m h^{-1} in beech saplings. These findings indicate that the degree of coupling between Δ_A and the respired CO_2 signal might not only be related to species, phenology and tree height but may also vary with environmental conditions.

Conclusions

This study demonstrates that the isotopic composition of CO_2 released by various components of the ecosystem may not reflect exactly the isotopic composition of the CO_2 fixed during photosynthesis. Should more experiments confirm our findings, it will be necessary to explore the impact of such results on $\delta^{13}C$ of atmospheric CO_2 and biomass C pools alongside their temporal variations using isotope-enabled vegetation models. To achieve this, it might be necessary to describe explicitly the isotopic mixing of recent photosynthates into a large plant C pool that provides the substrate for autotrophic respiration and biomass production. For example, some models based on such principles are used to interpret the intra-annual isotopic variations deposited in tree ring cellulose at high resolution (Ogée *et al.*, 2009). This approach seems promising and could be applied to the modelling of plant respiratory signals and exploration of the effects of various post-photosynthetic processes hypothesized in our study, especially the observed differences between the $\delta^{13}C$ of stem respired CO_2, phloem sugars and cellulose. However, because these processes seem to vary among species, there will be a need to conduct similarly detailed studies in other ecosystems to gauge and explain differences in isotopic patterns and their potential implications on the mass C balance of the plant and the atmosphere. With more studies such as the one presented here, future isotope-enabled soil-vegetation–atmosphere transfer models will be better able to develop and parameterize transfer functions that can account for these phenomenon and be used to interpret and predict the isotopic impact of biosphere gas exchange on $\delta^{13}C$ of atmospheric CO_2.

Acknowledgements

This work was supported with salary for LW through a EU-FP6 grant (CarboEurope-IP) awarded to JG, an ANR grant (MIST) awarded to JO and a Marie Curie Intra-European Career Development Fellowship awarded to LW. Research leading to these results has received funding from the European Community's Seventh Framework Programme (FP7/2007-2013) under grant agreement no. 237582. Additional funding support for the experiment were provided by the Région Aquitaine through a grant awarded to Céline Meredieu, the ORE FORET through a grant awarded to DL and the INRA department EFPA through a grant awarded to JO. We thank Michel Sartore, Cathy Lambrot and Andy Cross for their laboratory and field assistance. We also thank Andy Cross for providing data on the litter and soil C isotope composition, Michel Stievenard, Monique Pierre and Anais Feron for analysing the wood cellulose C isotype composition and Jean Marc Bonnefond, Didier Garigou and Sandra Debesa for providing meteorological and eddy covariance flux data. Furthermore, we would like to thank Martina Schmidt (LSCE), Willi Brand, Armin Jordan and Michel Rothe (Max Planck Institute for Biogeochemistry), along with the IMECC structure for their support and assistance with our calibration needs. Lastly we would like to thank Dave Bowling and Jaleh Ghashghaie for helpful discussions.

References

Andrews JA, Matamala R, Westover KM, Schlesinger WH. 2000. Temperature effects on the diversity of soil heterotrophs and the $\delta^{13}C$ of soil-respired CO_2. *Soil Biology and Biochemistry* **32**: 699–706.

Aranibar JN, Berry JA, Riley WJ, Pataki DE, Law BE, Ehleringer JR. 2006. Combining meteorology, eddy fluxes, isotope measurements, and modeling to understand environmental controls of carbon isotope discrimination at the canopy scale. *Global Change Biology* **12**: 710–730.

Badeck F, Fontaine J-L, Dumas F, Ghashghaie J. 2009. Consistent patterns in leaf lamina and leaf vein carbon isotope composition across ten herbs and tree species. *Rapid Communications in Mass Spectrometry* **23**: 2455–2460.

Badeck F-W, Tcherkez G, Nogués S, Piel C, Ghashghaie J. 2005. Post-photosynthetic fractionation of stable carbon isotopes between plant organs – a widespread phenomenon. *Rapid Communications in Mass Spectrometry* **19**: 1381–1391.

Bahn M, Schmitt M, Siegwolf RTW, Richter A, Brüggemann N. 2009. Does photosynthesis affect grassland soil-respired CO_2 and its carbon isotope composition on a diurnal timescale. *New Phytologist* **182**: 451–460.

Bakwin PS, Tans PP, White JWC, Andres RJ. 1998. Determination of the isotopic ($^{13}C/^{12}C$) discrimination by terrestrial biology from a global network of observations. *Global Biogeochemical Cycles* **12**: 555–562.

Baldocchi DD, Bowling DR. 2003. Modelling the discrimination of $^{13}CO_2$ above and within a temperate broad-leaved forest canopy on hourly to seasonal time scales. *Plant, Cell & Environment* **26**: 231–244.

Barbour MM, Hunt JE, Dungan RJ, Turnbull MH, Brailsford GW, Farquhar GD, Whitehead D. 2005. Variation in the degree of coupling between $\delta^{13}C$ of phloem sap and ecosystem respiration in two mature *Nothofagus* forests. *New Phytologist* **166**: 497–512.

Bathellier C, Badeck F, Couzi P, Harscoet S, Mauve C, Ghashghaie J. 2007. Divergence in $d^{13}C$ of dark respired CO_2 and bulk organic matter occurs during the transition between heterotrophy and autotrophy in *Phaseolus vulgaris* L. plants. *New Phytologist* **177**: 406–418.

Bathellier C, Tcherkez G, Bligny R, Gout E, Cornic G, Ghashghaie J. 2008. Metabolic origin of the $\delta^{13}C$ of respired CO_2 in roots of *Phaseolus vulgaris*. *New Phytologist* **181**: 387.

Battle M, Bender M, Tans PP, White JWC, Ellis JT, Conway T, Francey RJ. 2000. Global carbon sinks and their variability inferred from atmospheric O_2 and $\delta^{13}C$. *Science* **287**: 2467–2470.

Berbigier P, Bonnefond J-M, Mellmann P. 2001. CO_2 and water vapour fluxes for 2 years above Euroflux forest site. *Agricultural and Forest Meteorology* **108**: 183–197.

Bert D, Danjon F. 2006. Carbon concentration variations in the roots, stem and crown of mature *Pinus pinaster* (Ait.). *Forest Ecology and Management* **222**: 279–295.

Bhupinderpal-Singh, Nordgren A, Ottosson Löfvenius M, Högberg MN, Mellander PE, Högberg P. 2003. Tree root and soil heterotrophic respiration as revealed by girdling of boreal Scots pine forest: extending observations beyond the first year. *Plant, Cell & Environment* **26**: 1287–1296.

Bowling DR, McDowell NG, Bond BJ, Law BE, Ehleringer JR. 2002. ^{13}C content of ecosystem respiration is linked to precipitation and vapor pressure deficit. *Oecologia* **131**: 113–124.

Bowling DR, Pataki DE, Richardson JT. 2008. Carbon isotopes in terrestrial ecosystem pools and CO_2 fluxes. *New Phytologist* **178**: 24–40.

Brandes E, Kodama N, Whittaker K, Weston C, Rennenberg H, Keitel C, Adams MA, Gessler A. 2006. Short-term variation in the isotopic composition of organic matter allocated from the leaves to the stem of *Pinus sylvestris*: effects of photosynthetic and post-photosynthetic carbon isotope fractionation. *Global Change Biology* **12**: 1922–1939.

Cernusak LA, Marshall JD, Comstock JP, Balster NJ. 2001. Carbon isotope discrimination in photosynthetic bark. *Oecologia* **128**: 24–35.

Cernusak LA, Pate JS, Farquhar GD. 2002. Diurnal variation in the stable isotope composition of water and dry matter in fruiting *Lupinus angustifolius* under field conditions. *Plant, Cell & Environment* **25**: 893–907.

Cernusak LA, Tcherkez G, Keitel C, Cornwell WK, Santiago LS, Knohl A, Barbour MM, Williams DG, Reich PB, Ellsworth DS *et al.* 2009. Why are non-photosynthetic tissues generally ^{13}C-enriched compared with leaves in C_3 plants? Review and synthesis of current hypotheses. *Functional Plant Biology* **36**: 199–213.

Ciais P, Tans PP, Trolier M, White JWC, Francey RJ. 1995. A large northern hemisphere terrestrial CO_2 sink indicated by the $^{13}C/^{12}C$ ratio of atmospheric CO_2. *Science* **269**: 1098–1102.

Damesin C, Lelarge C. 2003. Carbon isotope composition of current-year shoots from *Fagus sylvatica* in relation to growth, respiration and use of reserves. *Plant, Cell & Environment* **26**: 207–219.

Delzon S, Sartore M, Granier A, Loustau D. 2004. Radial profiles of sap flow with increasing tree size in maritime pine. *Tree Physiology* **24**: 1285–1293.

Devaux M, Ghashghaie J, Bert D, Lambrot C, Gessler A, Bathellier C, Ogée J, Loustau D. 2009. Carbon stable isotope ratio of phloem sugars in mature pine trees throughout the growing season: comparison of two extraction methods. *Rapid Communications in Mass Spectrometry* **23**: 2511–2518.

Dieuaide-Noubhani M, Raffard G, Canioni P, Pradet A, Raymond P. 1995. Quantification of compartmented metabolic fluxes in maize root tips using isotope distribution from ^{13}C- or ^{14}C-labelled glucose. *The Journal of Biological Chemistry* **270**: 13147–13159.

Ekblad A, Boström B, Holm A, Comstedt D. 2005. Forest soil respiration rate and $d^{13}C$ is regulated by recent above ground weather conditions. *Oecologia* **143**: 136–142.

Ekblad A, Högberg P. 2001. Natural abundance of ^{13}C in CO_2 respired from forest soils reveals speed of link between tree photosynthesis and root respiration. *Oecologia* **127**: 305–308.

Farquhar GD, Ehleringer JR, Hubick KT. 1989. Carbon isotope discrimination and photosynthesis. *Annual Review of Plant Physiology and plant Molecular Biology* **40**: 503–537.

Farquhar GD, O'Leary MH, Berry JA. 1982. On the relationship between carbon isotope discrimination and the intercellular carbon dioxide concentration in leaves. *Australian Journal of Plant Physiology* **9**: 121–137.

Francey RJ, Tans PP, Allison CE, Enting IG, White JWC, Trolier M. 1995. Changes in oceanic and terrestrial carbon uptake since 1982. *Nature* **373**: 326–330.

Gessler A, Keitel C, Kodama N, Weston C, Winters AJ, Keith H, Grice K, Leuning R, Farquhar GD. 2007. $\delta^{13}C$ of organic matter transported from the leaves to the roots in *Eucalyptus delegatensis*: short-term variations and relation to respired CO_2. *Functional Plant Biology* **34**: 692–706.

Gessler A, Tcherkez G, Karyanto O, Keitel C, Ferrio JP, Ghashghaie J, Kreuzwieser J, Farquhar GD. 2009. On the metabolic origin of the carbon isotope composition of CO_2 evolved from darkened light-acclimated leaves in *Ricinus communis*. *New Phytologist* **181**: 374–386.

Gessler A, Tcherkez G, Peuke AD, Ghashghaie J, Farquhar GD. 2008. Experimental evidence for diel variations of the carbon isotope composition in leaf, stem and phloem sap organic matter in *Ricinus communis*. *Plant, Cell & Environment* **31**: 941–953.

Gleixner G, Danier H-J, Werner RA, Schmidt H-L. 1993. Correlations between the ^{13}C content of primary and secondary plant products in different cell compartments and that in decomposing Basidiomycetes. *Plant Physiology* **102**: 1287–1290.

Gleixner G, Schmidt H-L. 1997. Carbon isotope effects on the fructose-1,6-bisphosphate aldolase reaction, origin for non-statistical ^{13}C

distributions in carbohydrates. *The Journal of Biological Chemistry* **272**: 5382–5387.

Granier A, Loustau D. 1994. Measuring and modelling the transpiration of a maritime pine canopy from sap-flow data. *Agricultural and Forest Meteorology* **71**: 61–81.

Griffis TJ, Sargent SD, Baker JM, Lee X, Tanner BD, Greene J, Swiatek E, Billmark KA. 2008. Direct measurement of biosphere–atmosphere isotopic CO_2 exchange using the eddy covariance technique. *Journal of Geophysical Research* **113**. doi: 10.1029/2007JD009297.

Högberg P, Högberg MN, Göttlicher SG, Betson NR, Keel SG, Metcalfe DB, Campbell C, Schindlbacher A, Hurry V, Lundmark T *et al.* 2008. High temporal resolution tracing of photosynthate carbon from the tree canopy to forest soil microorganisms. *New Phytologist* **177**: 220–228.

Hu J, Moore DJP, Monson RK. 2010. Weather and climate controls over the seasonal carbon isotoped dynamics of sugars from subalpine forest trees. *Plant, Cell & Environment* **33**: 35–47.

Kaplan JO, Prentice IC, Buchmann N. 2002. The stable carbon isotope composition of the terrestrial biosphere: modeling at scales from the leaf to the globe. *Global Biogeochemical Cycles* **16**: 1060.

Keeling CD. 1961. The concentration and isotopic abundances of carbon dioxide in rural and marine air. *Geochimica et Cosmochimica Acta* **24**: 277–298.

Keitel C, Adams MA, Holst T, Matzarakis A, Mayer H, Rennenberg H, Gessler A. 2003. Carbon and oxygen isotope composition of organic compounds in the phloem sap provides a short-time measure for stomatal conductance of European beech (*Fagus sylvativa*). *Plant, Cell & Environment* **26**: 1157–1168.

Klumpp K, Schäufele R, Lötscher M, Lattanzi FA, Feneis W, Schnyder H. 2005. C-isotope composition of CO_2 respired by shoots and roots: fractionation during dark respiration? *Plant, Cell & Environment* **28**: 241–250.

Knohl A, Werner RA, Brand W, Buchmann N. 2005. Short-term variations in $\delta^{13}C$ of ecosystem respiration reveals link between assimilation and respiration in a deciduous forest. *Oecologia* **142**: 70–82.

Kodama N, Barnard RL, Salmon Y, Weston C, Ferrio JP, Holst J, Werner RA, Saurer M, Rennenberg H, Buchmann N *et al.* 2008. Temporal dynamics of the carbon isotope composition in a *Pinus sylvestris* stand: from newly assimilated organic carbon to respired carbon dioxide. *Oecologia*. doi: 10.1007/s00442-008-1030-1.

Kozlowski TT. 1992. Carbohydrates sources and sinks in woody plants. *The Botanical Review* **58**: 107–222.

Lai CT, Ehleringer JR, Schauer AJ, Tans PP, Hollinger DY, Paw UKT, Munger JW, Wofsy SC. 2005. Canopy-scale $\delta^{13}C$ of photosynthetic and respiratory CO_2 fluxes: observations in forest biomes across the United States. *Global Change Biology* **11**: 633–643.

Lloyd J, Farquhar GD. 1994. ^{13}C discrimination during CO_2 assimilation by the terrestrial biosphere. *Oecologia* **99**: 201–215.

Marron N, Plain C, Longdoz B, Epron D. 2009. Seasonal and daily time course of the ^{13}C composition in soil CO_2 efflux recorded with a tunable diode laser spectrophotometer (TDLS). *Plant and Soil* **318**: 137–151.

Maseyk K, Wingate L, Seibt U, Ghashghaie J, Bathellier C, Almeida P, Lobo de Vale R, Pereira JS, Yakir D, Mencuccini M. 2009. Biotic and abiotic factors affecting the d13C of soil respired CO2 in a Mediterranean oak woodland. *Isotopes in Environmental and Health Studies* **45**: 343–359.

McDowell NG, Bowling DR, Bond BJ, Irvine J, Law BE, Anthoni P, Ehleringer JR. 2004. Response of the carbon isotopic content of ecosystem, leaf, and soil respiration to meteorological and physiological driving factors in a *Pinus ponderosa* ecosystem. *Global Biogeochemical Cycles* **18**: GB1013, doi:10.1029/2003GB002049.

McNevin DB, Badger MR, Kane HJ, Farquhar GD. 2006. Measurement of (carbon) kinetic isotope effect by Rayleigh fractionation using membrane inlet mass spectrometry for CO_2-consuming reactions. *Functional Plant Biology* **33**: 1115–1128.

Melzer E, O'Leary MH. 1987. Anapleurotic CO_2 fixation by phosphoenolpyruvate carboxylase in C_3 plants. *Plant Physiology* **84**: 58–60.

Mencuccini M, Hölttä T. 2009. The significance of phloem transport for the speed with which canopy photosynthesis and belowground respiration are linked. *New Phytologist* **185**: 189–203.

Miller J, Tans PP. 2003. Calculating isotopic fractionation from atmospheric measurements at various scales. *Tellus* **55**: 207–214.

Mortazavi B, Chanton JP. 2002. Carbon isotopic discrimination and control of nighttime canopy $\delta^{18}O$-CO_2 in a pine forest in the southeastern United States. *Global Biogeochemical Cycles* **16**: 1008. 1010.1029/2000GB001390.

Mortazavi B, Chanton JP, Prater JL, Oishi AC, Oren R, Katul G. 2005. Temporal variability in ^{13}C of respired CO_2 in a pine and a hardwood forest subject to similar climatic conditions. *Oecologia* **142**: 57–69.

Münch E. 1930. *Die stoffbewgungen in der Pflanze*. Jena, Germany: Gustav Fischer.

Neuberger DS, Evert RF. 1974. Structure and development of the sieve-element protoplast in the hypocotyl of *Pinus resinosa*. *American Journal of Botany* **61**: 360–374.

Nguyen A, Lamant A. 1988. Pinitol and myo-inositol accumulation in water-stressed seedlings of Maritime pine. *Phytochemistry* **27**: 3423–3427.

Ogée J, Barbour MM, Wingate L, Bert D, Bosc A, Stievenard M, Lambrot C, Pierre M, Bariac T, Loustau D *et al.* 2009. A single-substrate model to interpret intra-annual stable isotope signals in tree ring cellulose. *Plant, Cell & Environment* **32**: 1071–1090. doi:1010.1111/j.1365-3040.2009.01989.x.

Ogée J, Brunet Y, Loustau D, Berbigier P, Delzon S. 2003a. MuSICA, a CO_2, water and energy multilayer, multileaf pine forest model: evaluation from hourly to yearly time scales and sensitivity analysis. *Global Change Biology* **9**: 697–717.

Ogée J, Peylin P, Ciais P, Bariac T, Brunet Y, Berbigier P, Roche C, Richard P, Bardoux G, Bonnefond J-M. 2003b. Partitioning net ecosystem exchange into net assimilation and respiration using $^{13}CO_2$ measurements: a cost-effective sampling strategy. *Global Biogeochemical Cycles* **17**: GB1070, doi: 1010.1029/2002GB001995.

Ogée J, Peylin P, Cuntz M, Bariac T, Brunet Y, Ciais P. 2004. Partitioning net ecosystem carbon exchange into net assimilation and respiration with canopy-scale isotopic measurements: an error propagation analysis with $^{13}CO_2$ and $CO^{18}O$ data. *Global Biogeochemical Cycles* **18**: GB2019, doi: 2010.1029/2003GB002166.

Peuke AD, Windt C, Van As H. 2006. Effects of cold-girdling on flows in the transport phloem in *Ricinus communis*: is mass flow inhibited? *Plant, Cell & Environment* **29**: 15–25.

Plain C, Gerant D, Maillard P, Dannoura M, Dong Y, Zeller B, Priault P, Parent F, Epron D. 2009. Tracing of recently assimilated carbon in respiration at high temporal resolution in the field with a tuneable diode laser absorption spectrometer after *in situ* $^{13}CO_2$ pulse labelling of 20-year-old beech trees. *Tree Physiology* **29**: 1433–1445.

Porté A, Bosc A, Champion I, Loustau D. 2000. Estimating the foliage area of maritime pine (*Pinus pinaster* Aït.) branches and crowns with application to modelling the foliage area distribution in the crown. *Annals of Forest Science* **57**: 73–86.

Porté A, Loustau D. 1998. Variability of the photosynthetic characteristics of mature needles within the crown of a 25-year old *Pinus pinaster*. *Tree physiology* **18**: 223–232.

Ramonet M, Ciais P, Nepomniachii I, Sidorov K, Neubert REM, Langendorfer U, Picard D, Kazan V, Biraud S, Gusti M *et al.* 2002. Three years of aircraft-based trace gas measurements over the

Fyodorovskoye southern taiga forest, 300 km north-west of Moscow. *Tellus* **54B**: 713–734.

Randerson JT, Collatz GJ, Fessenden JE, Munoz AD, Still CJ, Berry JA, Fung I, Suits N, Denning AS. 2002. A possible global covariance between terrestrial gross primary production and ^{13}C discrimination: consequences for the atmospheric ^{13}C budget and its response to ENSO. *Global Biogeochemical Cycles* **16**. doi:10.1029/2001GB001845.

Rossman A, Butzenlechner M, Schmidt H-L. 1991. Evidence for a nonstatistical carbon isotope distribution in natural glucose. *Plant Physiology* **96**: 609–614.

Ruehr NK, Offermann CA, Gessler A, Winkler JB, Ferrio JP, Buchmann N, Barnard RL. 2009. Drought effects on allocation of recent carbon: from beech leaves to soil CO_2 efflux. *New Phytologist* **184**: 950–961.

Schaeffer SM, Anderson DE, Burns SP, Monson RK, Sun J, Bowling DR. 2008. Canopy structure and atmospheric flows in relation to the $\delta^{13}C$ of respired CO_2 in a subalpine coniferous forest. *Agricultural and Forest Meteorology* **148**: 592–605.

Schulz A. 1992. Living sieve cells of conifers as visualized by confocal, laser-scanning fluorescence microscopy. *Protoplasma* **166**: 153–164.

Schulz A, Thompson GA. 2001. Phloem structure and function. *Encyclopedia of Life Sciences*. doi: 10.1002/9780470015902.a9780470001290.pub9780470015902.

Smith AE, Phillips DV. 2010. Influence of sequential prolonged periods of dark and light on pinitol concentration in clover and soybean tissue. *Physiologia Plantarum* **54**: 31–33.

Steinmann K, Siegwolf RTW, Saurer M, Körner C. 2004. Carbon fluxes to the soil in a mature temperate forest assessed by ^{13}C isotope tracing. *Oecologia* **141**: 489–501.

Subke J-A, Vallack HW, Magnusson T, Keel SG, Metcalfe DB, Högberg P, Ineson P. 2009. Short-term dynamics of abiotic and biotic soil $^{13}CO_2$ effluxes after *in situ* $^{13}CO_2$ pulse labelling of a boreal pine forest. *New Phytologist* **183**: 349–357.

Sun W, Resco V, Williams DG. 2009. Diurnal and seasonal variation in the carbon isotope composition of leaf dark-respired CO_2 in velvet mesquite (*Prosopis velutina*). *Plant, Cell & Environment* **32**: 1390–1400.

Tcherkez G, Farquhar GD, Badeck F-W, Ghashghaie J. 2004. Theoretical considerations about carbon isotope distribution in glucose of C_3 plants. *Functional Plant Biology* **31**: 857–877.

Tcherkez G, Nogués S, Bleton J, Cornic G, Badeck F, Ghashghaie J. 2003. Metabolic origin of carbon isotope composition of leaf dark-respired CO_2 in French bean. *Plant Physiology* **131**: 237–244.

Wingate L. 2008. Weighty issues in respiratory metabolism: intriguing carbon isotope signals from roots and leaves. *New Phytologist* **177**: 285–287.

Wingate L, Ogee J, Burlett R, Bosc A. 2010. Strong seasonal disequilibrium measured between the oxygen isotope signals of leaf and soil CO_2 exchange. *Global Change Biology*. doi: 10.1111/j.1365-2486.2010.02186.x.

Wingate L, Seibt U, Maseyk K, Ogee J, Almeida P, Yakir D, Pereira JS, Mencuccini M. 2008. Oxygen stable isotope signals of net soil CO_2 efflux record changes in soil evaporation and indicate the presence of carbonic anhydrase in Mediterranean soils. *Global Change Biology* **14**: 2178–2193.

Wingate L, Seibt U, Moncrieff J, Lloyd J, Berry J. 2007. Variations in ^{13}C discrimination during CO_2 exchange in *Picea sitchensis* branches in the field. *Plant, Cell & Environment* **30**: 600–616. doi: 610.1111/j.1365-3040.2007.01647.x.

Zobitz JM, Keener JP, Schnyder H, Bowling DR. 2006. Sensitivity analysis and quantification of uncertainty for isotopic mixing relationships in carbon cycle research. *Agricultural and Forest Meteorology* **136**: 56–75.

Supporting Information

Additional supporting information may be found in the online version of this article.

Fig. S1 Typical sampling sequence used in this study.

Fig. S2 Normalised 1-Hz time-series of isotopologue concentrations and ratios.

Fig. S3 Checking for memory effects.

Fig. S4 Normalized distributions of standard errors on calibration measurements.

Methods S1 Extended methods section.

Table S1 Characteristics of reference CO_2, calibration tanks and vacuum times

Table S2 Mean standard errors for the site average scan for different data types

Please note: Wiley-Blackwell are not responsible for the content or functionality of any supporting information supplied by the authors. Any queries (other than missing material) should be directed to the *New Phytologist* Central Office.